APCOM'07 in conjunction with EPMESC XI, December 3-6, 2007, Kyoto, JAPAN

A Direct Procedure for the Transient Analysis of Dynamic Soil-Structure Interaction Problems

Suriyon Prempramote[1*], Mohammad H. Bazyar[1], Chongmin Song[1]

[1]*School of Civil and Environmental Engineering, University of New South Wales, Sydney, NSW 2052, Australia*
e-mail: suriyon@student.unsw.edu.au, mhbazyar@student.unsw.edu.au, c.song@unsw.edu.au

Abstract A direct procedure for the transient analysis of dynamic soil-structure interaction problems is developed based on some recent advances in the scaled boundary finite-element method. Applying the continued-fraction solution of the scaled boundary finite-element equation in dynamic stiffness, the equations of motion of both bounded and unbounded domains are formulated as that in classical structural dynamics, i.e., a system of ordinary differential equations with time-independent coefficient matrices. No convolution integral is present. This formulation permits the application of standard time-stepping schemes to perform a transient analysis. The technique of reduced set of base functions is employed to further increase the computational efficiency. A numerical example demonstrates the simplicity in mesh generation, accuracy and efficiency of the novel solution procedure.

Key words: Scaled boundary finite-element method; Dynamic soil-structure interaction; Transmitting boundary; Super-element; Structural dynamics.

INTRODUCTION

A structure interacts with the supporting soil under dynamic actions, such as earthquakes and impacts. The structure is of finite dimension and usually modeled by the finite element method. The inertial effect of a finite element is modeled by a mass matrix, which represents the low frequency behavior. To model the high frequency response, the mesh has to be refined leading to a larger number of degrees of freedom. In comparison with the size of the structure, soil is assumed to cover an unbounded domain. The dynamic analysis of an unbounded domain is a difficult task, especially when it is performed directly in the time domain. Many numerical methods have been developed for this purpose. The boundary element method [1] satisfies the governing equations in the problem domain and the radiation condition at infinity automatically by using a fundamental solution. Only the boundary needs to be discretized. However, the fundamental solution is very complicated to evaluate when the material is anisotropic. In a direct time domain analysis, a convolution integral has to be computed. Various approximate transmitting boundaries have been proposed [2], but they have to be applied at a large distance from the structure and may suffer from instability problem. Recently, high-order transmitting boundaries, i.e. [3], have been proposed for scalar waves, but their extension to vector waves is a challenging task.

The scaled boundary finite-element method provides an alternative in the analysis of dynamic soil-structure interaction problems. Only the boundary is discretized as in the boundary element method, but no fundamental solution is required. General anisotropic materials can be analyzed without additional efforts. This method has been applied successfully in frequency and time domains, e.g, [4, 5]. Recently, a continued-fraction solution of the scaled boundary finite-element equation in dynamic stiffness has been obtained for both bounded and unbounded domains [6, 7]. The equation of motion is expressed in static stiffness, damping and mass matrices as in classical structural dynamics. As a result, standard numerical procedures in structural dynamics are applicable to perform dynamic soil-structure interaction problems. In this paper, a direct procedure for the transient analysis based on this novel solution procedure is presented by combining the solution procedures for bounded and unbounded domains.

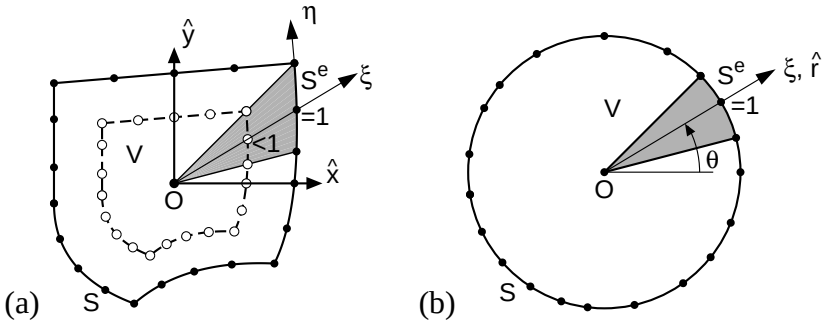

Figure 1. Scaled boundary coordinates: (a) scaling center O, radial coordinate ξ and boundary discretization; (b) geometry of transformed domain

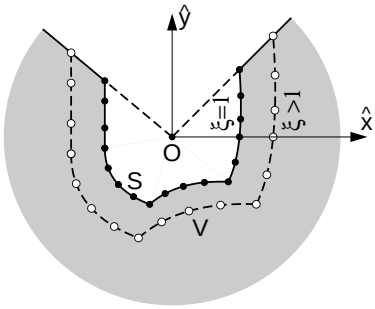

Figure 2. Representation of unbounded domain in scaled boundary coordinates

SUMMARY OF THE SCALED BOUNDARY FINITE-ELEMENT METHOD

The derivation of the scaled boundary finite-element equation and the continued-fraction solution are detailed in Refs. [8, 9] and [7], respectively. Only the key concept and equations are summarized.

In the scaled boundary finite-element method [8, 9], a so-called scaling center O is chosen in a zone from which the total boundary S is visible. A bounded domain V is shown in Figure 1(a) as an example. Without losing generality, the origin of the Cartesian coordinate system $\hat{x}$, $\hat{y}$ is selected at the scaling center. The boundary S is discretized into elements. The coordinates of the nodes of an element in the Cartesian coordinate system are arranged in $\{x\}$, $\{y\}$. The geometry of an element is interpolated using the shape functions $[N(\eta)]$ formulated in the local coordinate η. The geometry of the domain V is described by scaling the boundary with the dimensionless radial coordinate ξ pointing from the scaling center O to a point on the boundary. $\xi = 0$ at O and $\xi = 1$ on the boundary are chosen (Figure 1(a)). A point $(\hat{x}, \hat{y})$ inside the domain is thus expressed as

$$\hat{x}(\xi,\eta) = \xi x(\eta) = \xi [N(\eta)]\{x\}; \qquad \hat{y}(\xi,\eta) = \xi y(\eta) = \xi [N(\eta)]\{y\} \tag{1}$$

The coordinates ξ, η are called the *scaled boundary coordinates*. They resemble the polar coordinates $\hat{r}$ and θ. When the origin of a polar coordinate system coincides with the scaling center as in Figure 1(b), the polar coordinates are expressed using Eq. (1) as

$$\hat{r}(\xi,\eta) = \xi r(\eta); \qquad \theta(\eta) = \arctan(y(\eta)/x(\eta)) \tag{2}$$

where $r(\eta) = \sqrt{x^2(\eta) + y^2(\eta)}$ is the radial coordinate on the boundary. As the whole boundary is visible from the scaling center, $\theta(\eta)$ is a single-valued function in its principal value ($-\pi < \theta \leq \pi$). The element number and the local coordinate η can be regarded as a discrete representation of the angle θ. In the scaled boundary coordinates, The boundary S of the problem domain V is described by a constant radial coordinate $\xi = 1$ as shown in Figure 1(b). A bounded domain V is thus specified by $0 \leq \xi \leq 1$.

Unbounded domains can be conveniently defined by constant values of the scaled boundary coordinates. An example is shown in Figure 2. The scaling center O is chosen at the intersection between the straight free surfaces. Only the part of boundary directly visible from the scaling center is discretized. The straight surfaces passing through the scaling center are defined by constant values of η and are not discretized. The unbounded domain is thus specified by $1 \leq \xi \leq \infty$.

Along radial lines passing through the scaling center O and a node on the boundary, the nodal displacement functions $\{u(\xi)\}$ are introduced (For simplicity, the dependency on time t or the excitation frequency ω is omitted from the argument when it is not explicitly required). The nodal displacements on the boundary follow as $\{u\} = \{u(\xi = 1)\}$. Isoparametric displacement elements are used in the circumferential direction to interpolate the displacement functions piecewisely

$$\{u(\xi,\eta)\} = [N^u(\eta)]\{u(\xi)\} = [N_1(\eta)[I],\, N_2(\eta)[I], \ldots]\{u(\xi)\} \tag{3}$$

where $[I]$ is a 2×2 identity matrix.

The scaled boundary finite-element equation is derived by applying the Galerkin's weighted residual technique or the virtual work method in the circumferential direction η to the governing differential equations. In the frequency domain, the *scaled boundary finite-element equation in displacement* is expressed as

$$[E^0]\xi^2\{u(\xi)\}_{,\xi\xi}+([E^0]-[E^1]+[E^1]^T)\xi\{u(\xi)\}_{,\xi}-[E^2]\{u(\xi)\}+(\omega\xi)^2[M^0]\{u(\xi)\}=0 \qquad (4)$$

where ω is the excitation frequency. $[E^0]$, $[E^1]$, $[E^2]$ and $[M^0]$ are coefficient matrices obtained by assembling the element coefficient matrices as in the finite element method. The element coefficient matrices are available in Ref. [10]. The coefficient matrices $[E^0]$ and $[M^0]$ are positive-definite. $[E^2]$ is symmetric. As for the mass matrices in finite elements, $[E^0]$ and $[M^0]$ can be lumped to the nodes [11]. $[E^0]$ will be a block-diagonal matrix consisting blocks of the size 2×2 . $[M^0]$ will be a diagonal matrix. The techniques of using Gauss-Lobatto-Legendre shape functions and quadrature to obtain lumped $[E^0]$ and $[M^0]$ are investigated in [11].

The internal nodal forces along the radial lines are obtained by integrating the surface traction over elements. They are expressed as

$$\{q(\xi)\} =[E^0]\xi\{u(\xi)\}_{,\xi}+[E^1]^T\{u(\xi)\} \qquad (5)$$

The internal nodal forces are related to the nodal forces on the boundary of a domain. For a bounded domain defined by a boundary with a constant ξ, the outward normal is the same as the positive direction of the radial coordinate ξ in the scaled boundary coordinates. Introducing the definition of the dynamic stiffness matrix $[S(\omega,\xi)]$, the nodal forces are expressed as

$$\{R(\xi)\}=\{q(\xi)\}=[S(\omega,\xi)]\{u(\xi)\} \qquad (6)$$

Eliminating $\{q(\xi)\}$ and $\{u(\xi)\}$ from Eqs. (4), (5) and (6) leads to an equation for the dynamic stiffness matrix $[S(\omega,\xi)]$ [8]. Formulated on the boundary ($\xi=1$), the scaled boundary finite-element equation for the dynamic stiffness matrix of a bounded domain $[S(\omega)]=[S(\omega,\xi=1)]$ is written as

$$([S(\omega)]-[E^1])[E^0]^{-1}([S(\omega)]-[E^1]^T)-[E^2]+\omega[S(\omega)]_{,\omega}+\omega^2[M^0]=0 \qquad (7)$$

A similar equation can be derived for an unbounded domain. Note that the outward normal of an unbounded domain is pointing towards the scaling center. The dynamic-stiffness matrix $[S^\infty(\omega,\xi)]$ (superscript ∞ for unbounded) is defined by

$$\{R(\xi)\}=-\{q(\xi)\}=[S^\infty(\omega,\xi)]\{u(\xi)\} \qquad (8)$$

The scaled boundary finite-element equation in dynamic stiffness is written on the boundary ($\xi=1$) of an unbounded domain as

$$([S^\infty(\omega)]+[E^1])[E^0]^{-1}([S^\infty(\omega)]+[E^1]^T)-\omega[S^\infty(\omega)]_{,\omega}-[E^2]+\omega^2[M^0]=0 \qquad (9)$$

MODELING OF UNBOUNDED DOMAIN BASED ON CONTINUED-FRACTION SOLUTION FOR DYNAMIC STIFFNESS MATRIX

An analytical solution in frequency domain is developed in [12] for the scaled boundary finite-element equation in displacement (Eq. (4)). It is expressed as matrix functions of the excitation frequency. To satisfy the radiation condition at infinity, an asymptotic solution has to be applied. This solution can not be used in combination with well-established methods in structural dynamics to perform a direct time domain analysis. To overcome this difficulty, a continued-fraction solution of the scaled boundary finite-element equation (Eq. (9)) for the dynamic stiffness matrix of an unbounded domain is developed in [6].

This new solution leads to the development of a high-order transmitting boundary. The key equations are summarized in the following.

An order M_{cf}^{∞} continued-fraction solution of the dynamic stiffness matrix $[S^{\infty}(\omega)]$ is expressed as

$$[S^{\infty}(\omega)] = \mathrm{i}\omega[C_{\infty}] + [K_{\infty}] - (\mathrm{i}\omega[Y_1^{(1)}] + [Y_0^{(1)}] - (\mathrm{i}\omega[Y_1^{(2)}] + [Y_0^{(2)}] - \ldots - (\mathrm{i}\omega[Y_1^{(M_{\mathrm{cf}}^{\infty})}] + [Y_0^{(M_{\mathrm{cf}}^{\infty})}])^{-1} \ldots)^{-1})^{-1} \quad (10)$$

The first two terms are the dashpot matrix $[C_{\infty}]$ and the spring matrix $[K_{\infty}]$. $[Y_1^{(i)}]$ and $[Y_0^{(i)}]$ $(i = 1, 2, \ldots M_{\mathrm{cf}}^{\infty})$ are the coefficient matrices of the high-order terms. These coefficient matrices of the continued-fraction solution are determined by substituting Eq. (10) into Eq. (9).

The solution for $[C_{\infty}]$ satisfying the radiation condition is symmetric and positive definite (assuming a time dependence of $e^{+\mathrm{i}\omega t}$)

$$[C_{\infty}] = [E^0][\Phi]\,\lceil\Lambda\rfloor\,[\Phi]^T[E^0] \quad (11a)$$

where $\lceil\Lambda\rfloor$ are the positive square roots of the eigenvalues of the general eigenvalue problem

$$[M^0][\Phi] = [E^0][\Phi]\,\lceil\Lambda^2\rfloor \quad (11b)$$

The eigenvector matrix $[\Phi]$ is normalized as

$$[\Phi]^T[E^0][\Phi] = [I] \quad (11c)$$

When $[E^0]$ and $[M^0]$ are lumped, Eq. (11b) is a series of independent eigenvalue problems of size 2×2. $[\Phi]$ and $[C_{\infty}]$ are also block-diagonal with the same structure. The spring matrix is equal to

$$[K_{\infty}] = [E^0][\Phi][k_{\infty}][\Phi]^T[E^0] \quad (12a)$$

where $[k_{\infty}]$ is the solution of

$$\lceil\Lambda\rfloor[k_{\infty}] + [k_{\infty}]\,\lceil\Lambda\rfloor = -\lceil\Lambda\rfloor\,[\Phi]^T[E^1]^T[\Phi] - [\Phi]^T[E^1][\Phi]\,\lceil\Lambda\rfloor + \lceil\Lambda\rfloor \quad (12b)$$

The coefficient matrices of the high-order terms $[Y_1^{(i)}]$ and $[Y_0^{(i)}]$ $(i = 1, 2, \ldots M_{\mathrm{cf}}^{\infty})$ are determined recursively. Defining the constant matrices for the case $i = 1$

$$[a^{(1)}] = [E^0]^{-1} \quad (13a)$$

$$[b_0^{(1)}] = [E^0]^{-1}([K_{\infty}] + [E^1]^T) \quad (13b)$$

$$[V^{(1)}] = [\Phi] \quad (13c)$$

$$[c^{(1)}] = ([K_{\infty}] + [E^1])[E^0]^{-1}([K_{\infty}] + [E^1]^T) - [E^2] \quad (13d)$$

The solution for $[Y_1^{(i)}]$ is determined from

$$[Y_1^{(i)}]^{-1} = [V^{(i)}]^{-T}[y_1^{(i)}]^{-1}[V^{(i)}]^{-1} \quad (14a)$$

where $[y_1^{(i)}]^{-1}$ is the solution of

$$[y_1^{(i)}]^{-1}\,\lceil\Lambda\rfloor + \lceil\Lambda\rfloor\,[y_1^{(i)}]^{-1} = [V^{(i)}]^T[c^{(i)}][V^{(i)}] \quad (14b)$$

The solution for $[Y_0^{(i)}]$ is obtained as

$$[Y_0^{(i)}] = [V^{(i+1)}]^{-T}[y_0^{(i)}][V^{(i+1)}]^{-1} \quad (15a)$$

where $[V^{(i+1)}]$ is given in Eq. (16c) and $[y_0^{(i)}]$ is the solution of

$$\lceil\Lambda\rfloor[y_0^{(i)}]+[y_0^{(i)}]\lceil\Lambda\rfloor=[V^{(i+1)}]^T[b_0^{(i)}][V^{(i)}]+[V^{(i)}]^T[b_0^{(i)}]^T[V^{(i+1)}]+[y_1^{(i)}]^{-1} \tag{15b}$$

Introducing the recursive formula for the coefficient matrices

$$[a^{(i+1)}]=[c^{(i)}] \tag{16a}$$
$$[b_0^{(i+1)}]=-[b_0^{(i)}]^T+[c^{(i)}][Y_0^{(i)}] \tag{16b}$$
$$[V^{(i+1)}]=[Y_1^{(i)}]^{-1}[V^{(i)}] \tag{16c}$$
$$[c^{(i+1)}]=[a^{(i)}]-[b_0^{(i)}][Y_0^{(i)}]-[Y_0^{(i)}][b_0^{(i)}]^T+[Y_0^{(i)}][c^{(i)}][Y_0^{(i)}] \tag{16d}$$

$[Y_1^{(i)}]$ and $[Y_0^{(i)}]$ are determined by applying Eqs. (14) and (15) repeatedly to the specified order M_{cf}^{∞} with the constant matrices updated by using Eq. (16).

On the boundary of an unbounded domain, the nodal force $\{R(\omega)\}=\{R(\omega,\xi=1)\}$- nodal displacement $\{u(\omega)\}=\{u(\omega,\xi=1)\}$ relationship is obtained by formulating Eq. (8) at $\xi=1$ and using Eq. (10)

$$\{R(\omega)\}=(\mathrm{i}\omega[C_\infty]+[K_\infty]-(\mathrm{i}\omega[Y_1^{(1)}]+[Y_0^{(1)}]-(\mathrm{i}\omega[Y_1^{(2)}]+[Y_0^{(2)}])^{-1}-\ldots \\ -(\mathrm{i}\omega[Y_1^{(M_{\mathrm{cf}}^{\infty})}]+[Y_0^{(M_{\mathrm{cf}}^{\infty})}])^{-1}\ldots)^{-1})^{-1}\{u(\omega)\} \tag{17}$$

This equation can be reformulated by introducing auxiliary variables as

$$([K_{\mathrm{h}}^{\infty}]+(\mathrm{i}\omega)[C_{\mathrm{h}}^{\infty}])\{y(\omega)\}=\{F(\omega)\} \tag{18}$$

with the function $\{y(\omega)\}$, the external excitation $\{F(\omega)\}$ and the frequency-independent coefficient matrices $[K_{\mathrm{h}}^{\infty}]$, $[C_{\mathrm{h}}^{\infty}]$ defined as (The column concatenation is denoted by semicolons)

$$\{y(\xi)\}=\{\{u(\xi)\};\{u^{(1)}(\xi)\};\{u^{(2)}(\xi)\};\ldots\{u^{(M_{\mathrm{cf}}^{\infty}-1)}(\xi)\};\{u^{(M_{\mathrm{cf}}^{\infty})}(\xi)\}\} \tag{19a}$$
$$\{F(\xi)\}=\{\{R(\xi)\};0;0;\ldots;0;0\} \tag{19b}$$
$$[K_{\mathrm{h}}^{\infty}]=\begin{bmatrix} [K_\infty] & -[I] & 0 & \cdots & 0 & 0 \\ -[I] & [Y_0^{(1)}] & -[I] & \cdots & 0 & 0 \\ 0 & -[I] & [Y_0^{(2)}] & \cdots & 0 & 0 \\ \vdots & \vdots & \vdots & \ddots & -[I] & 0 \\ 0 & 0 & 0 & -[I] & [Y_0^{(M_{\mathrm{cf}}^{\infty}-1)}] & -[I] \\ 0 & 0 & 0 & 0 & -[I] & [Y_0^{(M_{\mathrm{cf}}^{\infty})}] \end{bmatrix} \tag{19c}$$
$$[C_{\mathrm{h}}^{\infty}]=\mathrm{diag}([C_\infty],\ [Y_1^{(1)}],\ [Y_1^{(2)}],\ \cdots\ [Y_1^{(M_{\mathrm{cf}}^{\infty}-1)}],\ [Y_1^{(M_{\mathrm{cf}}^{\infty})}]) \tag{19d}$$

where $\{u^{(i)}(\xi)\}$ ($i=1,2,\ldots,M_{\mathrm{cf}}$) are auxiliary variables. It can be verified by eliminating the auxiliary variables that Eq. (17) is equivalent to Eq. (18) with Eq. (19). Equation (18) is a standard equation of motion of a linear system in structural dynamics written in the frequency domain. It is expressed in the time domain as a high-order temporally local transmitting boundary condition

$$[K_{\mathrm{h}}^{\infty}]\{y(t)\}+[C_{\mathrm{h}}^{\infty}]\{\dot{y}(t)\}=\{F(t)\} \tag{20}$$

The continued-fraction solution and the resulting high-order transmitting boundary condition can be used in combination with the reduced set of base functions [13]. The size of the system of equations is reduced to the number of base functions retained in the reduced set. A parametric study on the order of continued fraction is given in [6].

MODELING OF BOUNDED DOMAIN BASED ON CONTINUED-FRACTION SOLUTION FOR DYNAMIC STIFFNESS

The continued-fraction solution can also be constructed for a bounded domain [7]. The inertial effect is modeled by increasing the order of the continued fraction without an internal mesh. The equations for implementation are given in [14] in the same mini-symposium. Only the conclusion will be stated in this paper.

For a bounded domain, an order M_{cf} continued-fraction solution of the dynamic stiffness is expressed on the boundary ($\xi = 1$) as

$$[S(\omega)] = [K] - \omega^2[M] - \omega^4([S_0^{(1)}] - \omega^2[S_1^{(1)}] - \omega^4([S_0^{(2)}] - \omega^2[S_1^{(2)}] - \ldots - \omega^4([S_0^{(M_{\mathrm{cf}})}] - \omega^2[S_1^{(M_{\mathrm{cf}})}])^{-1}\ldots)^{-1})^{-1} \quad (21)$$

where $[K]$ and $[M]$ are the static stiffness and mass matrices, respectively. They represent the low frequency expansion of the dynamic stiffness matrix and are routinely used in structural dynamics. $[S_0^{(i)}]$ and $[S_1^{(i)}]$ ($i = 1, 2, \ldots, M_{\mathrm{cf}}$) are coefficient matrices of the high-order terms, which represent the high frequency response. These coefficient matrices can be determined by substituting Eq. (21) into Eq. (7). The equation of motion on the boundary of a bounded domain is expressed as

$$([K_{\mathrm{h}}] - \omega^2[M_{\mathrm{h}}])\{y(\omega)\} = \{F(\omega)\} \quad (22)$$

with

$$\{y(\omega)\} = \{\{u(\omega)\}; \{u^{(1)}(\omega)\}; \{u^{(2)}(\omega)\}; \ldots \{u^{(M_{\mathrm{cf}})}(\omega)\}\} \quad (23a)$$

$$\{F(\omega)\} = \{\{R(\omega)\}; 0; 0; \ldots 0\} \quad (23b)$$

$$[K_{\mathrm{h}}] = \mathrm{diag}([K],\, [S_0^{(1)}],\, [S_0^{(2)}],\, \cdots,\, [S_0^{(M_{\mathrm{cf}})}]) \quad (23c)$$

$$[M_{\mathrm{h}}] = \begin{bmatrix} [M] & -[I] & 0 & \cdots & 0 \\ -[I] & [S_1^{(1)}] & -[I] & \cdots & 0 \\ 0 & -[I] & [S_1^{(2)}] & \cdots & 0 \\ \vdots & \vdots & \vdots & \ddots & \vdots \\ 0 & 0 & 0 & \cdots & [S_1^{(M_{\mathrm{cf}})}] \end{bmatrix} \quad (23d)$$

where $\{u^{(i)}(\xi)\}$ ($i = 1, 2, \ldots, M_{\mathrm{cf}}$) are auxiliary variables. In the time domain, Eq. (22) is written as

$$[K_{\mathrm{h}}]\{y(t)\} + [M_{\mathrm{h}}]\{\ddot{y}(t)\} = \{F(t)\} \quad (24)$$

NUMERICAL EXAMPLE

Starting from the continued-fraction solution, equations of motion of both bounded domains and unbounded domains are expressed as linear equations with frequency- or time-independent coefficient matrices. In the substructure technique of dynamic soil-structure interaction analysis, the equations of motion of the substructures can be assembled as in the finite element method. Direct coupling with standard finite elements is also straightforward when the same shape functions are employed at the common boundary. The resulting equation of motion for the global system can be solved by standard procedures in structural dynamics. In a time-domain analysis, time stepping techniques such as Newmark method can be used.

A frame-like structure [15] shown in Figure 3(a) is analyzed as an example to illustrate the effect of dynamic soil-structure interaction and to demonstrate the simplicity and accuracy of the novel solution procedure of the scaled boundary finite-element equation. Plane stress condition is considered. The analyses are performed directly in the time domain by using the Newmark method with $\gamma = 0.5$ and $\beta = 0.25$. A consistent set of units is used in the analysis. The dimensions of the structure are given in the figure. The

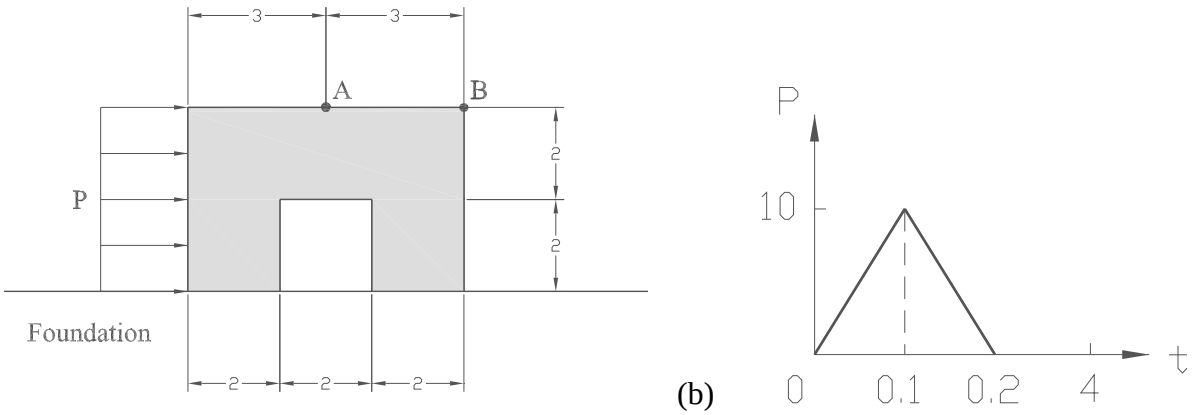

Figure 3. Frame-like structure: (a) Geometry; (b) Time history of impulse loading

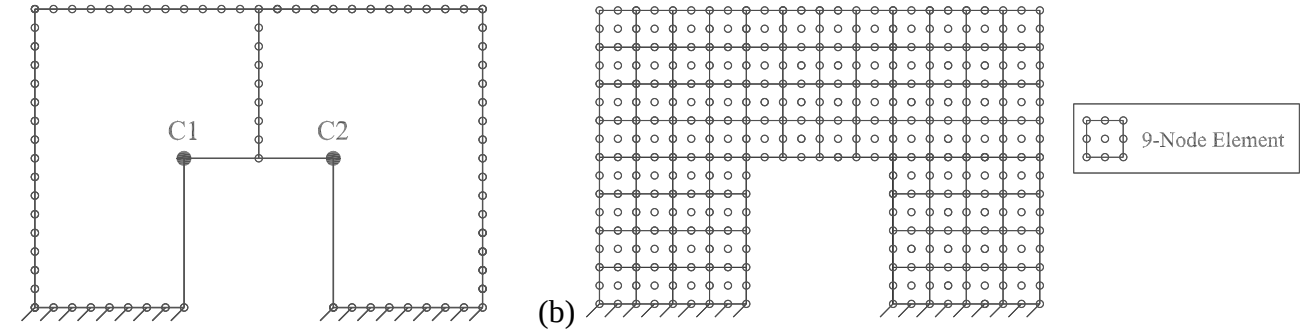

Figure 4. Frame-like structure on rigid foundation: (a) Scaled boundary finite-element mesh; (b) Finite element mesh

material properties are defined by the modulus of elasticity $E = 10^4$, Poisson's ratio $\nu = 0.2$ and the density of mass $\rho = 1$. A pressure impulse with an amplitude of 10 is applied to the left side of the structure. The time history of the impulse is shown in Figure 3(b).

To evaluate the effect of dynamic soil-structure interaction on the response of this frame-like structure, both a rigid foundation and a flexible foundation are considered. In the case of the rigid foundation, the base of the structure is assumed to be fixed. In the scaled boundary finite-element analysis, two subdomains are introduced (Figure 4(a)). The scaling centers are chosen at the two inner corners C1 and C2. The boundaries of the subdomains are discretized with 3-node elements. The order of the continued fraction is chosen as $M_{\text{cf}} = 3$. The time step is selected as $\Delta t = 0.01$. A finite element analysis is performed using a commercial software package ADINA to provide a reference solution. The mesh of 9-node finite elements is shown in Figure 4(b). The density of the finite element mesh on the boundary is the same as the scaled boundary finite-element mesh. The horizontal displacements at Points A and B are plotted in Figure 5. The present scaled boundary finite-element result agrees very well with the finite element result obtained from ADINA.

In the case of the flexible foundation, it is assumed that the structure is resting on a half-plane with the same material properties. The scaled boundary finite-element mesh is shown in Figure 6. A part of the unbounded domain surrounding the structure is modeled as three bounded subdomains. The scaling centers are located at the centers of the subdomains. The order of continued fraction is chosen as $M_{\text{cf}} = 3$. The remaining part of the half-plane is modeled as an unbounded domain. Its scaling center is chosen at C1.

A scaled boundary finite-element analysis with the length $L = 5$ (Figure 6) is performed. A reduced set of 14 based functions are selected. The order of continued fraction is chosen as $M_{\text{cf}}^{\infty} = 5$. The horizontal displacement response at Point A is plotted in Figure 7(a). To provide a reference solution, an extended finite element mesh is analyzed using ADINA. In the extended mesh, $L = 60$ (Figure 6) is chosen. The outer boundary is fixed. The dilatational wave generated by the impulse loading will be reflected back to the shear wall at about $t = 1.2$. The horizontal displacement response at Point A is shown in Figure 7(a).

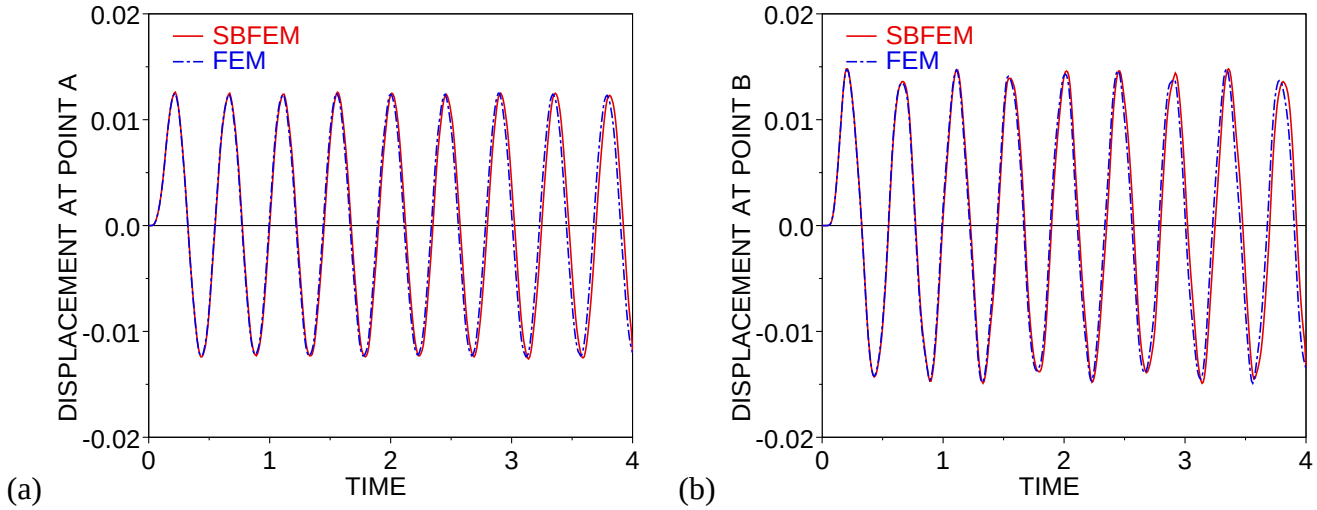

Figure 5. Horizontal displacements of frame-like structure on rigid foundation: (a) Point A; (b) Point B

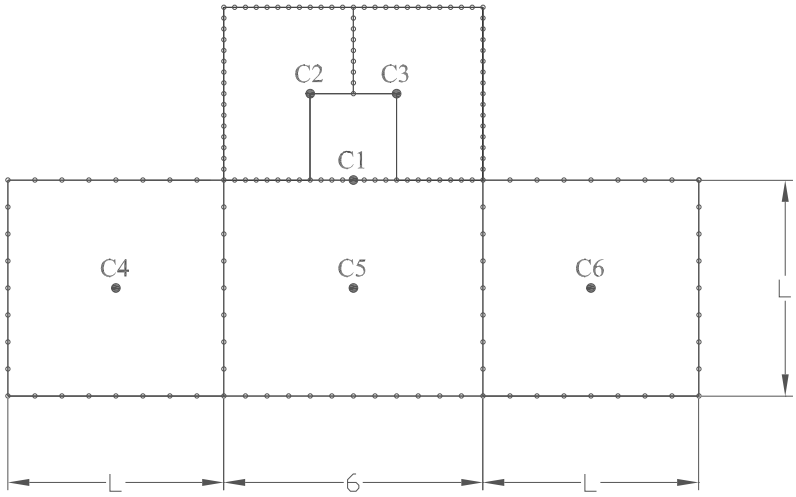

Figure 6. Frame-like structure on flexible half plane

It is observed that the two results agree well before the waves reflected at the outer boundary of the extended mesh reach the structure. To further verify the result, a scaled boundary finite-element analysis is perform with $L = 10$ (Figure 6), which increases the distance between the structure and the boundary of the unbounded domain. As shown in Figure 7(b), the result is very close to that for $L = 5$.

It is observed by comparing Figure 5(a) with Figure 7(b) that the dynamic interaction between the structure and the foundation strongly affects the structure response. When the dynamic soil-structure interaction is considered for this example, the maximum displacement response increases due to the flexibility of the unbounded domain. The amplitude of the response increases, too. The radiation damping of the unbounded domain leads to rapid decay of the vibration (Figure 7(b)). This phenomenon does not occur when the foundation is rigid (Figure 5(a)).

CONCLUSIONS

A procedure to perform a dynamic soil-structure interaction analysis directly in the time domain is presented. A structure-soil system is divided into bounded and unbounded subdomains. Each subdomain is modeled by using the scaled boundary finite-element method. A new continued-fraction solution of the scaled boundary finite-element method is applied. The equation of motion of an unbounded domain is expressed in a high-order static stiffness matrix and a high-order damping matrix, and that of a bounded domain in a high-order static stiffness matrix and a high-order mass matrix. Newmark method is applied to

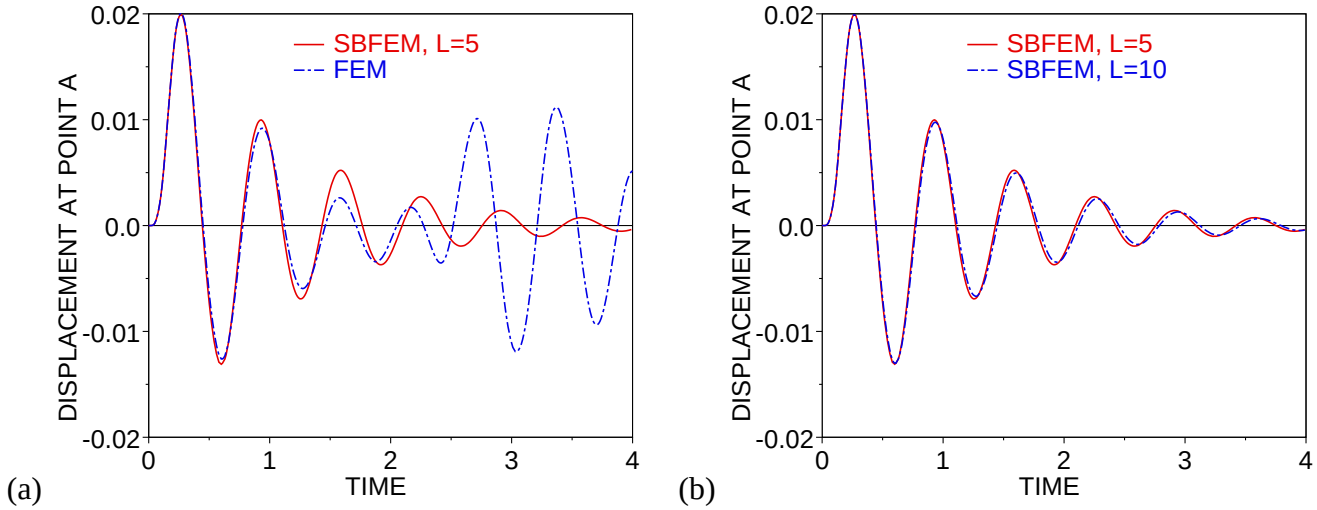

Figure 7. Horizontal displacement at point A of frame-like structure on flexible foundation: (a) $L = 5$; (b) $L = 10$

perform the time integration. As only the boundary of the subdomains is discretized, the mesh generation is simpler than in the finite element method. This also reduces the size of the equation of motion of the global system. A numerical example is presented to illustrate the simplicity of this direct procedure.

References

[1] W. S. Hall and G. Oliveto. *Boundary Element Methods for Soil-Structure Interaction*. Kluwer Academic Publishers, 2003.

[2] J. P. Wolf. *Soil-Structure-Interaction Analysis in Time Domain*. Prentice-Hall, Englewood Cliffs, 1988.

[3] T. Hagstrom and T. Warburton. A new auxiliary variable formulation of high-order local radiation boundary condition: corner compatibility conditions and extensions to first-order systems. *Wave Motion*, 39:327–338, 2004.

[4] J. Y. Yan, C. H. Zhang, and F. Jin. A coupling procedure of FE and SBFE for soil-structure interaction in the time domain. *International Journal for Numerical Methods in Engineering*, 59:1453–1471, 2004.

[5] L. Lehmann and T. Ruberg. Application of hierarchical matrices to the simulation of wave propagation in fluids. *Communications in Numerical Methods in Engineering*, 22:489–503, 2006.

[6] M. H. Bazyar and Ch. Song. A continued-fraction-based high-order transmitting boundary for wave propagation in unbounded domains of arbitrary geometry. *International Journal for Numerical Methods in Engineering*, in press.

[7] Ch. Song. The scaled boundary finite-element method in structural dynamics. *International Journal for Numerical Methods in Engineering*, submitted for review.

[8] Ch. Song and J. P. Wolf. The scaled boundary finite-element method – alias consistent infinitesimal finite-element cell method – for elastodynamics. *Computational Methods in Applied Mechanics and Engineering*, 147:329–355, 1997.

[9] J. P. Wolf and Ch. Song. The scaled boundary finite-element method – a primer: derivations. *Computers & Structures*, 78:191–210, 2000.

[10] J. P. Wolf and Ch. Song. *Finite-Element Modelling of Unbounded Media*. John Wiley & Sons, Chichester, 1996.

[11] Ch. Song and M. H. Bazyar. A fundamental-solution-less boundary element method for exterior wave problems. *Communication for Numerical Methods in Engineering*, in press.

[12] Ch. Song and J. P. Wolf. The scaled boundary finite-element method: analytical solution in frequency domain. *Computational Methods in Applied Mechanics and Engineering*, 164:249–264, 1998.

[13] Ch. Song. Dynamic analysis of unbounded domains by a reduced set of base functions. *Computational Methods in Applied Mechanics and Engineering*, 195:4075–4094, 2006.

[14] Ch. Song. Evaluation of dynamic stress intensity factors and T-stress using the scaled boundary finite-element method. In *Proceedings of APCOM'07 in conjunction with EPMESC XI*, Kyoto, JAPAN, December 3-6, 2007.

[15] Z. J. Yang and A. J. Deeks. A frequency-domain approach for modelling transient elastodynamics using scaled boundary finite element method. *Computational Mechanics*, 40:725–738, 2007.